RSC Advances

PAPER

View Article Online
View Journal | View Issue

Cite this: *RSC Adv.*, 2017, **7**, 30453

An antimalarial drug, tafenoquine, as a fluorescent receptor for ratiometric detection of hypochlorite†

Avijit Kumar Das,[a] Naoto Hayashi,[a] Yasuhiro Shiraishi *[ab] and Takayuki Hirai[a]

Received 1st May 2017
Accepted 6th June 2017

DOI: 10.1039/c7ra04867j

rsc.li/rsc-advances

Tafenoquine (**TQ**), a fluorescent antimalarial drug, was used as a receptor for the fluorometric detection of hypochlorite (OCl^-). **TQ** itself exhibits a strong fluorescence at 476 nm, but OCl^--selective cyclization of its pentan-1,4-diamine moiety creates a blue-shifted fluorescence at 361 nm. This ratiometric response facilitates rapid, selective, and sensitive detection of OCl^- in aqueous media with physiological pH. This response is also applicable to a simple test kit analysis and allows fluorometric OCl^- imaging in living cells.

Introduction

Hypochlorous acid (HOCl) is one of the most biologically important reactive oxygen species (ROS).[1] Its deprotonation at a physiological pH produces hypochlorite anions (OCl^-),[2] which act as a microbicidal agent in the immune system.[3] OCl^- is produced *in vivo* by the reaction of hydrogen peroxide (H_2O_2) and Cl^- on myeloperoxidase (MPO), a heme enzyme expressed in activated leukocytes.[4] Controlled OCl^- generation is necessary to inhibit the invading microbes, although OCl^- also reacts with several biomolecules such as amino acids, proteins, and nucleosides.[5] In contrast, uncontrolled OCl^- generation causes several diseases such as neuron degeneration, arthritis, and cancer.[6] Analytical methods that quantitatively detect OCl^- and allow visual imaging of OCl^- in biological samples by simple pre-treatment and inexpensive instrumentation are therefore necessary.

Fluorometric analysis with OCl^--selective receptor is one promising method for this purpose since this facilitates simple quantification or imaging of OCl^- with a common fluorescence spectrometer or microscope.[7] A number of fluorescent receptors for OCl^- have been proposed;[8] however, many of them show single-wavelength emission whose intensity is strongly affected by several factors (instruments and receptor concentrations). In contrast, ratiometric receptors, which show a new emission in addition to the inherent one by the interaction with OCl^-, is more attractive because they allow simple quantification just by monitoring the intensities of two emissions, where the effects of several factors can be eliminated. There are, however, a few reports of ratiometric OCl^- receptors.[9] Exploitation of new receptor is therefore a challenge.

Tafenoquine (**TQ**) is a commercially-available antimalarial drug,[10] one derivative of a representative antimalarial drug, primaquine (**PQ**),[11] as shown in Scheme 1. **TQ** shows higher antimalarial activity than **PQ**[12] and has attracted increasing attention because it is also effective for the treatment of Leishmaniasis, a disease caused by protozoan parasites.[13] It is also reported that **TQ** produces some mitochondrial ROS *in vivo* such as superoxide anion (O_2^-), H_2O_2, hydroxide (OH^-), and OCl^-, which leads to apoptosis-like death of Leishmania.[14] In addition, **TQ** inherently shows a strong fluorescence due to its quinoline platform. The strong fluorescence, high water solubility, high cell permeability, and high ROS tolerance of **TQ** are the ideal properties for fluorometric ROS sensing.

Here we report that **TQ** behaves as a ratiometric fluorescent receptor for OCl^- detection. The **TQ** itself exhibits a strong cyan fluorescence at 476 nm. Selective reaction of **TQ** with OCl^- leads to cyclization of its pentan-1,4-diamine moiety (Scheme 1). This creates a new blue-shifted emission at 361 nm, while decreasing the original 476 nm emission. This ratiometric response facilitates rapid, selective, and sensitive detection of OCl^- in

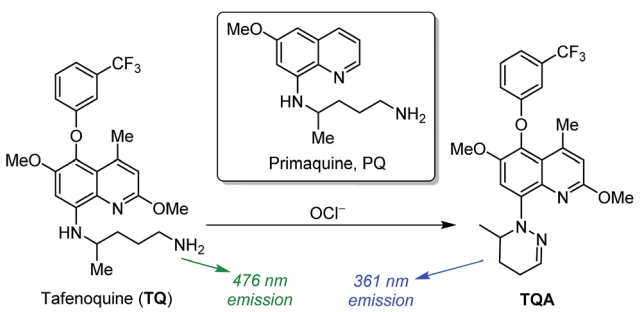

Scheme 1 Structures of 8-aminoquinoline-based antimalarial drugs, and proposed mechanism for OCl^--induced fluorescence response of **TQ**.

[a]*Research Center for Solar Energy Chemistry, Division of Chemical Engineering, Graduate School of Engineering Science, Osaka University, Toyonaka 560-8531, Japan. E-mail: shiraish@cheng.es.osaka-u.ac.jp*

[b]*Precursory Research for Embryonic Science and Technology (PRESTO), Japan Science and Technology Agency (JST), Saitama 332-0012, Japan*

† Electronic supplementary information (ESI) available: Supplementary data (Fig. S1–S10), and Cartesian coordinates for molecules. See DOI: 10.1039/c7ra04867j

solution and allows OCl^- imaging in living cells. This is the first report of **TQ** for application to sensory material.

Results and discussion

Fluorescence properties of TQ

TQ was obtained by neutralization of commercially-available succinate salt of tafenoquine with Na_2CO_3 as brown solids with 83% yield. Its purity was confirmed by ^1H, ^{13}C NMR and ESI-MS analysis (Fig. S1–S3, ESI†). The fluorescence response of **TQ** was studied in a buffered water/MeCN (3/7 v/v) mixture with pH 7.4 (HEPES 0.1 M) at 25 °C (λ_{ex} = 300 nm). As shown in Fig. 1a, **TQ** itself (20 μM) exhibits a strong fluorescence at 476 nm. Upon addition of 100 equiv. of OCl^- to the solution, a blue-shifted fluorescence appears at 361 nm ($\Delta\lambda$ = 115 nm), along with a decrease in the original 476 nm emission. To clarify the specific nature of **TQ** towards OCl^-, effect of other typically encountered oxidative species such as F^-, AcO^-, Cl^-, Br^-, I^-, NO_2^-, NO_3^-, SO_3^{2-}, PO_4^{3-}, OH^-, H_2O_2, SCN^-, hydroxyl radical ($^{\bullet}OH$), singlet oxygen ($^1O_2$), and NO was studied. As summarized in Fig. 1a, these species, when added to a solution containing **TQ**, scarcely change the fluorescence spectrum. This indicates that OCl^- selectively changes the fluorescence of **TQ**. It must also be noted that, as shown in Fig. 1b, the OCl^--induced fluorescence change is unaffected by the addition of these competing oxidative species. These findings clearly suggest that **TQ** selectively detects OCl^- in aqueous media even in the presence of these competing species.

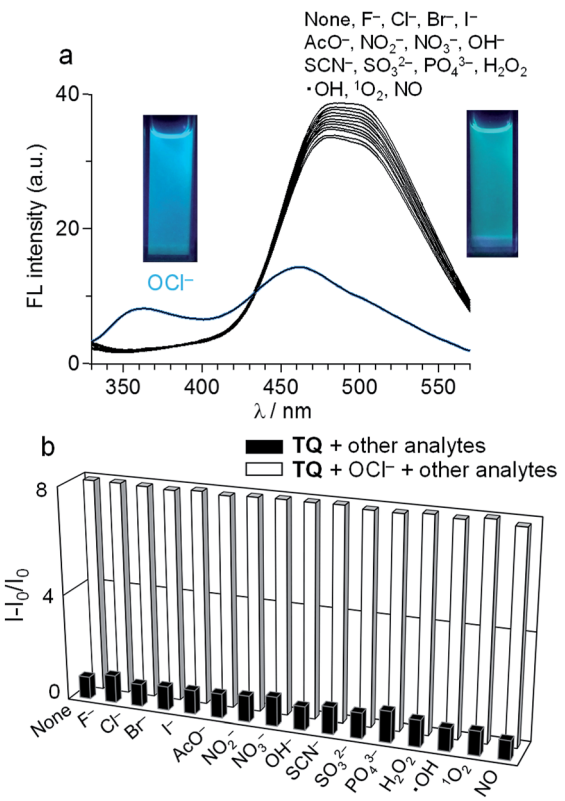

Fig. 1 (a) Fluorescence spectra (λ_{ex} = 300 nm) of **TQ** (20 μM) in a buffered water/MeCN (3/7 v/v) mixture (HEPES 0.1 M, pH 7.4) at 25 °C with 100 equiv. of each respective analytes. (b) Fluorescence intensity at 361 nm (black) with 100 equiv. of each respective analytes and (white) with 100 equiv. of each respective analytes together with 100 equiv. of OCl^-.

Fig. 2a shows the results of fluorescence titration of **TQ** with OCl^-. Stepwise addition of OCl^- creates a blue-shifted 361 nm emission together with a decrease in the 476 nm emission, with an isoemission point at 435 nm. This indicates that the reaction of **TQ** with OCl^- produces single component exhibiting the 361 nm emission. The fluorescence quantum yield of **TQ** is Φ = 0.39, while addition of 100 equiv. OCl^- decreases to Φ = 0.16. Fig. 2b shows the change in the ratio of emission intensities (I_{361}/I_{476}) with the OCl^- concentrations. The lower detection limit is determined to be 2.0 μM based on the signal-to-noise (S/N) ratio using the equation (DL = 3 × SD/S),[15] where SD is the standard deviation of blank analysis (SD = 2.4 × 10^{-3}, n = 8) and S is the slope of the intensity *versus* the OCl^- concentrations (S = 3.7 × 10^{-3} μM^{-1}). This detection limit is lower than the physiological OCl^- concentrations (5–25 μM) in the human body,[16] suggesting that **TQ** facilitates sensitive OCl^- detection. It must also be noted that **TQ** detects OCl^- very rapidly. Fig. S4 (ESI†) shows the time-dependent change in the fluorescence intensity of **TQ** after addition of OCl^-. The intensity change occurs immediately after OCl^- addition and almost terminates within 1 min, suggesting that only 1 min assay is enough for OCl^- sensing as is the case for previously reported receptors.[9] It is also noted that, as shown in Fig. S5 (ESI†), increase in the water content of solution decreases the intensity of OCl^--induced 361 nm emission; however, the intensity obtained with 90% water is *ca.* 50% as compared to the intensity obtained with 30% water. This indicates that **TQ** facilitates OCl^- sensing even in high water content solution.

Reaction of TQ with OCl^-

As shown in Scheme 2, the ratiometric emission response of **TQ** upon addition of OCl^- is ascribed to the transformation to **TQA**, *via* a formation of six-membered pyridiazine (1,2-diazine) ring by cyclization of the pentan-1,4-diamine moiety of **TQ**. This occurs based on basic and oxidizing properties of OCl^-. The OCl^- remove acidic protons of amine groups of **TQ** and give an anionic intermediate ($\mathbf{I_1}$). Subsequent oxidative

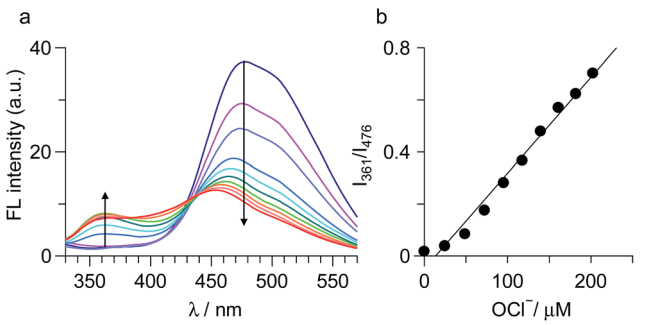

Fig. 2 (a) Change in fluorescence spectra of **TQ** (20 μM) upon titration with OCl^- in a buffered water/MeCN (3/7 v/v) mixture (HEPES 0.1 M, pH 7.4) at 25 °C. (b) Change in the ratio of fluorescence intensity of **TQ** (I_{361}/I_{476}) *versus* the OCl^- concentrations.

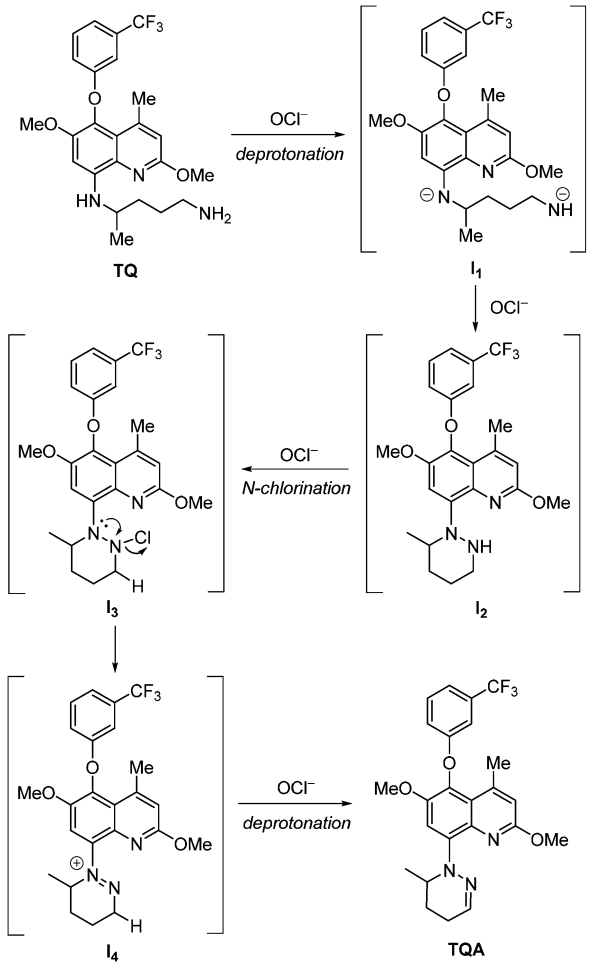

Scheme 2 Proposed mechanism for the reaction of **TQ** with OCl^-.

intramolecular coupling of the intermediate *via* an N–N bond formation[17] by OCl^- gives an azine-type intermediate ($\mathbf{I_2}$). Reaction of its azine nitrogen with OCl^- produces an *N*-chlorinated intermediate ($\mathbf{I_3}$). Elimination of Cl^- by an α-effect of lone pair on the adjacent nitrogen of hydrazino group gives a cyclic diazonium cation intermediate ($\mathbf{I_4}$). This then undergoes elimination of acidic β-hydrogen by OCl^- and produces **TQA**. The formation of **TQA** was clearly supported by ^1H and ^{13}C NMR and EI-MS analysis (Fig. S6–S8, ESI†). These findings indicate that the OCl^--induced transformation of **TQ** to **TQA** results in ratiometric fluorescence response (Fig. 2a).

It must be noted that pH of the solution is an important factor for OCl^- sensing by **TQ**. As shown in Fig. S9 (ESI†), the 361 nm fluorescence does not appear in acidic media (pH < 7) or basic media (pH > 10) even upon addition of OCl^-. In acidic media, protonation of OCl^- ($HOCl \rightleftarrows H^+ + OCl^-$; $pK_a = 7.6$)[18] decreases the basicity of OCl^- and, hence, suppresses the deprotonation step (**TQ** → $\mathbf{I_1}$). In contrast, basic media stabilize OCl^-, but suppress the oxidation step ($\mathbf{I_1} \rightarrow \mathbf{I_2}$). Therefore, fluorometric sensing of OCl^- using **TQ** is enabled in physiological pH media (7–10).

Mechanism for fluorometric response

TQ itself shows a strong fluorescence at a relatively longer wavelength (476 nm). This is ascribed to the electron donation from the secondary amine group at the 8-position to the electron deficient quinoline moiety. Upon addition of OCl^-, the resulting **TQA** shows a blue-shifted fluorescence at 361 nm. This is because the cyclization of the pentan-1,4-diamine moiety of **TQ** transforms the secondary amine moiety to the tertiary one, which has lower electron donation ability. This thus creates a blue-shifted emission.

To confirm the above mechanism for ratiometric emission response, *ab initio* calculations based on the density functional theory (DFT) were performed within the Gaussian 03 program. As shown in Table S1 (ESI†), singlet electronic transition of **TQ** mainly consists of HOMO → LUMO ($S_0 \rightarrow S_1$) transition. Its calculated transition energy (3.25 eV, 381 nm) is close to the absorption maximum (λ_{max}) of **TQ** observed at 375 nm (Fig. S10, ESI†). As shown in Fig. 3 (left), π-electrons of LUMO for **TQ** lie not only on the quinoline ring but also on the adjacent nitrogen atom at the 8-position. This suggests that strong electron donation from the secondary amine moiety of **TQ** to the quinoline moiety at the excited state creates longer-wavelength fluorescence at 476 nm.

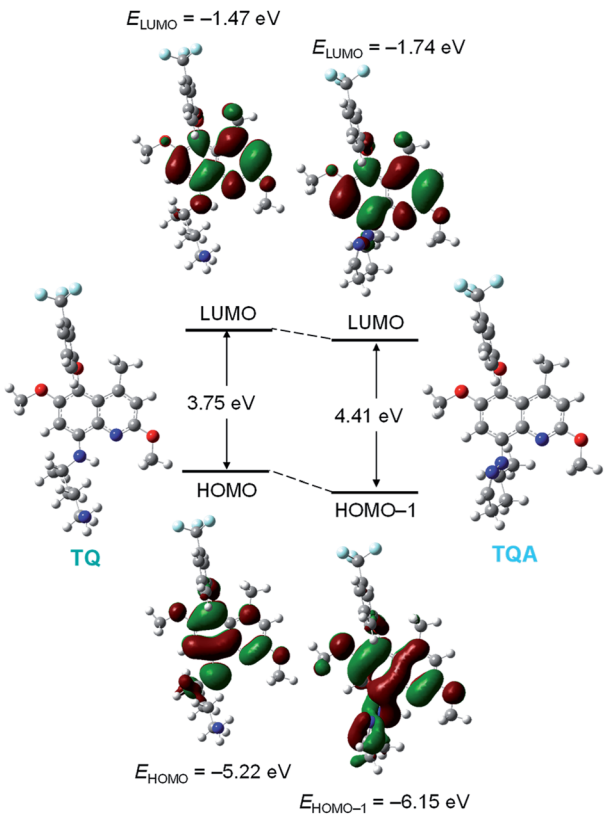

Fig. 3 Energy diagrams and electronic distribution for main molecular orbitals of (left) **TQ** and (right) **TQA**, calculated at the DFT level (B3LYP/6-31+G) using PCM with water as a solvent. Gray, white, blue, red and light blue atoms indicate C, H, N, O and F atoms, respectively. Green and deep red parts on the molecular orbitals refer to the different phases of molecular wave functions.

In the case of **TQA**, its singlet electronic transition is mainly contributed by HOMO−1 → LUMO ($S_0 \rightarrow S_3$) transition (Table S2, ESI†). Its calculated transition energy (3.84 eV, 322 nm) is close to λ_{max} of **TQA** (357 nm; Fig. S10, ESI†). As shown in Fig. 3 (right), π-electrons of LUMO for **TQA** lie mainly on the quinoline moiety, where the electrons are scarcely distributed on the nitrogen atom at the 8-position. These results indicate that **TQ** shows longer-wavelength fluorescence due to the electron donation from the secondary amine moiety; the cyclization of its pentan-1,4-diamine moiety by OCl^- suppresses the electron donation and exhibits blue-shifted fluorescence.

Test kit analysis

Prompted by high sensitivity and selectivity of **TQ** towards OCl^-, simple test strip kit loaded with **TQ** was prepared for practical applications.[19] The test strips were prepared by immersing a TLC plate (3 × 1 cm) into the **TQ** solution (200 μM, 5 mL) for 2 min followed by drying *in vacuo* for 12 h. The **TQ**-loaded test strips were added to solutions with different OCl^- concentrations for 2 min. The obtained strips were then photoirradiated with a 365 nm UV lamp. As shown in Fig. 4, these test strips clearly change their fluorescence color with the OCl^- concentrations. The test strip kit is therefore an useful qualitative tool for simple OCl^- analysis.

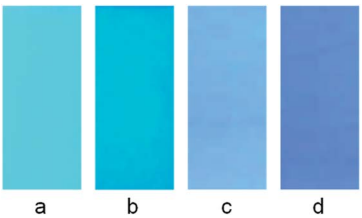

Fig. 4 Fluorescence color change of the TLC plate strips loaded with **TQ**. The respective pictures are (a) as-prepared TLC plate, and the plates obtained after addition to the solution containing (b) 200 μM, (c) 400 μM, and (d) 600 μM OCl^- for 2 min. All of the pictures were taken under photoirradiation of 365 nm lamp.

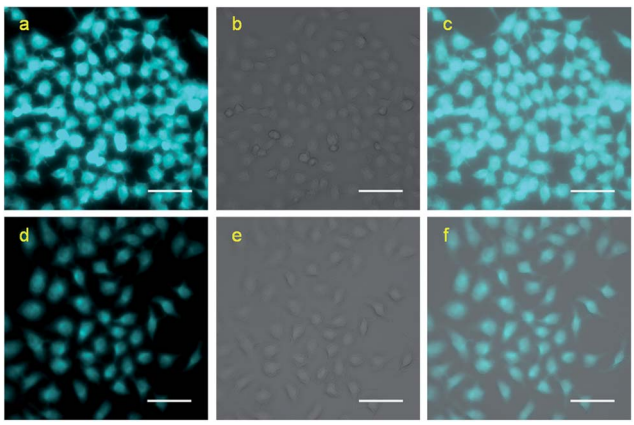

Fig. 5 Fluorescence images (λ_{ex} = 360 nm, λ_{em} = 460 nm) of HeLa cells incubated with 40 μM of **TQ** (a–c) without and (d–f) with 10 mM of OCl^-. (a and d) fluorescence image, (b and e) bright field image, and (c and f) merged images, respectively. The scale bars in all of the figures are set at 50 μm.

Cell imaging

To clarify the cell permeability of **TQ** and its applicability for practical imaging of OCl^- in living cells, biological experiments were performed using HeLa cells. The cells were incubated with **TQ** (40 μM) in DMSO at 37 °C under humidified air containing 5% CO_2, and washed with phosphate buffered saline (PBS). A PBS containing 10 mM of OCl^- was added to the cells, and the cells were incubated for 20 min. The cells were then washed with PBS, and their images were obtained by a fluorescence microscope. As shown in Fig. 5a, the cells incubated with **TQ**, when photoexcited at λ_{ex} = 360 nm, show strong fluorescence. However, as shown in Fig. 5d, the emission intensity is weakened significantly by the addition of OCl^- to the sample. These results clearly indicate that **TQ** successfully permeates through the plasma membrane of the cells and exhibits a fluorescence response toward OCl^- even in the living cells.

Conclusion

We demonstrated that an antimalarial drug, tafenoquine (**TQ**), behaves as a fluorescent receptor for ratiometric OCl^- detection. **TQ** shows strong fluorescence at 476 nm, but OCl^--selective cyclization of its pentan-1,4-diamine moiety creates a blue-shifted emission at 361 nm. This ratiometric response facilitates rapid, selective, and sensitive detection of OCl^- in aqueous media with physiological pH. This response is also applicable to a simple test kit analysis and allows fluorometric OCl^- imaging in living cells. The basic receptor design presented here based on the tafenoquine platform with high fluorescence quantum yield, high water solubility, high cell permeability, and high ROS tolerance may contribute to the design of more efficient fluorescent receptor for OCl^-.

Experimental

Materials and methods

All chemicals were used as received. $^{\bullet}OH$ was generated by the Fenton reaction.[20] $^1O_2$ was generated from the H_2O_2/MoO_4^{2-} system in alkaline media.[21] NO was generated using sodium nitroferricyanide(III) dihydrate.[22] ^1H and ^{13}C NMR charts were recorded on a JEOL JNM-ECS400 spectrometer with $CDCl_3$ using TMS as a standard. Mass analysis was performed on a JEOL JMS700 Mass Spectrometer. Absorption spectra were measured on an UV-visible photodiode-array spectrometer (Shimadzu; Multispec-1500) equipped with a temperature controller (S-1700).[23] Fluorescence spectra were measured on a JASCO FP-6500 fluorescence spectrophotometer with a 10 mm path length cell (both excitation and emission slit widths, 5.0 nm) at 298 ± 1 K using a temperature controller.[24] The pH titration was performed on Horiba pH Meter F-71. Fluorescence quantum yield (Φ_F) was determined with Rhodamine B (in EtOH) as a standard.[25]

Synthesis of TQ

Tafenoquine succinate salt (0.3 g, 0.52 mmol) was added to a water/CH_2Cl_2 (6/6 mL mL^{-1}) mixture. Water (6 mL) containing sodium carbonate (0.1 g, 0.94 mmol) was added to the mixture, and the mixture was stirred for 2 h at room temperature. The aqueous phase was extracted with CH_2Cl_2 (10 mL × 3). The combined organic phases were washed with water and concentrated by evaporation, affording **TQ** as brown solid (200 mg, yield 83%). ^{1}H NMR (300 MHz, $CDCl_3$, TMS) δ (ppm): 7.32 (q, 1H, J = 18 Hz), 7.21 (d, 1H, J = 6 Hz), 7.07 (s, 1H), 6.94 (d, 1H, J = 6 Hz), 6.64 (s, 1H), 6.50 (s, 1H), 5.84 (d, 1H, J = 6 Hz), 4.00 (s, 3H), 3.79 (s, 3H), 3.66 (s, 1H), 2.78 (d, 2H, J = 6 Hz), 2.55 (s, 3H), 1.69 (dd, 6H, J = 6 Hz, J = 9 Hz), 1.35 (d, 3H, J = 6 Hz). ^{13}C NMR (100 MHz, $CDCl_3$, TMS) δ (ppm): 159.64, 148.961, 146.339, 142.010, 132.085, 131.760, 131.007, 129.968, 126.917, 125.344, 122.636, 120.681, 118.006, 115.256, 112.052, 94.996, 56.989, 52.870, 48.446, 42.248, 34.439, 30.130, 23.103, 20.833. MS (m/z): M^+ calcd for $C_{24}H_{28}F_3N_3O_3$: 463.2083; found (ESI): 464.17 $(M + H)^+$.

Synthesis of TQA

TQ (0.2 g, 0.43 mmol) was dissolved in MeCN (50 mL) by vigorous stirring. Sodium hypochlorite (64 mg, 0.86 mmol) was added to the solution, and the solution was stirred at room temperature. The progress of the reaction was monitored with a TLC plate. After the reaction, MeCN was removed by evaporation, and the gummy product was purified by column chromatography using AcOEt/n-hexane (1/9 v/v) as an eluent, affording brown powders of **TQA** (130 mg, yield 65%). ^{1}H NMR (400 MHz, $CDCl_3$, TMS) δ (ppm): 7.438 (s, 1H), 7.284 (d, 1H, J = 6.4 Hz), 7.221 (m, 1H), 7.063 (s, 1H), 6.911 (m, 1H), 6.753 (s, 1H), 4.946 (q, 1H, J = 6.4 Hz), 3.999 (s, 3H), 3.787 (s, 3H), 3.728 (d, 1H, J = 1.2 Hz), 2.589 (s, 3H), 2.547 (s, 1H), 2.391 (t, 1H, J = 12.8 Hz), 2.302 (t, 1H, J = 4 Hz), 1.865 (d, 1H, J = 3.6 Hz), 0.992 (t, 3H, J = 6.8 Hz). ^{13}C NMR (100 MHz, $CDCl_3$, TMS) δ (ppm): 159.649, 159.011, 147.760, 146.196, 142.458, 138.797, 135.765, 133.677, 132.142, 130.936, 130.016, 121.329, 118.221, 115.422, 112.090, 111.809, 99.247, 56.598, 52.975, 50.677, 24.752, 23.255, 20.309, 13.959. MS (m/z): M^+ calcd for $C_{24}H_{24}F_3N_3O_3$: 459.177; found (EI^+): 459.

Calculation details

Ab initio calculations were performed with tight convergence criteria at the DFT level with the Gaussian 03 package, using the B3LYP/6-31+G basis set for all atoms. The excitation energies and oscillator strengths of the compounds were calculated by TDDFT[26] at the same level of optimization using the PCM with water as a solvent.[27] Cartesian coordinates are summarized at the end of this ESI.†

Cell culture and fluorescence microscopy

HeLa cells were grown in Dulbecco's modified Eagle's medium (DMEM) supplemented with 10% fetal bovine serum on cover slip in 60 mm dishes. The cells were incubated with **TQ** (40 μM, in DMSO). After washing three times with phosphate buffered saline (PBS), 10 mM of OCl^- (in PBS) was added and the cells were further incubated for 20 min. The cells then were washed three times with PBS and the imaging was carried out using BIOREVE BZ-9000 Fluorescence Microscope apparatus. All the cells were incubated at 37 °C in humidified air containing 5% CO_2.

Acknowledgements

We thank Dr Masaki Nakahata and Prof. Shinji Sakai (Graduate School of Engineering Science, Osaka University) for the use of fluorescence microscope. This work was supported by the Grant-in Aid for Scientific Research (No. 15K06556) from the Ministry of Education, Culture, Sports, Science and Technology, Japan (MEXT) and the Precursory Research for Embryonic Science and Technology (PRESTO, JPMJPR1442) from Japan Science and Technology Agency (JST).

Notes and references

1 A. Gomes, E. Fernandes and J. L. F. C. Lima, *J. Biochem. Biophys. Methods*, 2005, **65**, 45.
2 J. Shepherd, S. A. Hilderbrand, P. Waternan, J. W. Heinecke, R. Weissleder and P. Libby, *Chem. Biol.*, 2007, **14**, 1221.
3 A. J. Kettle and C. C. Winterbourn, *Redox Rep.*, 1997, **3**, 3.
4 T. Aokl and M. Munemorl, *Anal. Chem.*, 1983, **55**, 209.
5 S. L. Hazen, F. F. Hsu, K. Duffin and J. W. Heinecke, *J. Biol. Chem.*, 1996, **271**, 23080.
6 T. Sugiyama, M. Fujita, N. Koide and I. Mori, *Microbiol. Immunol.*, 2004, **48**, 957.
7 (*a*) Y. Zhou, J. Y. Li, K. H. Chu, K. Liu, C. Yao and J. Y. Li, *Chem. Commun.*, 2012, **48**, 4677; (*b*) Q. Xu, K. A. Lee, S. Lee, K. M. Lee, W. J. Lee and J. Yoon, *J. Am. Chem. Soc.*, 2013, **135**, 9944.
8 (*a*) X. Chen, F. Wang, J. Y. Hyun, T. Wei, J. Qiang, X. Ren, I. Shin and J. Yoon, *Chem. Soc. Rev.*, 2016, **45**, 2976; (*b*) S. Kenmoku, Y. Urano, H. Kojima and T. Nagano, *J. Am. Chem. Soc.*, 2007, **129**, 7313; (*c*) Y. Koide, Y. Urano, K. Hanaoka, T. Terai and T. Nagano, *J. Am. Chem. Soc.*, 2011, **133**, 5680; (*d*) X. Chen, X. Wang, S. Wang, W. Shi, K. Wang and H. Ma, *Chem.–Eur. J.*, 2008, **14**, 4719; (*e*) S. Goswami, A. K. Das, A. Manna, A. K. Maity, P. Saha, C. K. Quah, H. K. Fun and H. A. A. Aziz, *Anal. Chem.*, 2014, **86**, 6315; (*f*) P. Panizzi, M. Nahrendorf, M. Wildgruber, P. Waterman, J. L. Figueiredo and E. Aikawa, *J. Am. Chem. Soc.*, 2009, **131**, 15739; (*g*) Y. K. Yang, H. J. Cho, J. Lee, I. Shin and J. Tae, *Org. Lett.*, 2009, **11**, 859; (*h*) Y. Zhou, J. Y. Li, K. H. Chu, K. Liu, C. Yao and J. Y. Li, *Chem. Commun.*, 2012, **48**, 4677.
9 (*a*) G. Chen, F. Song, J. Wang, Z. Yang, S. Sun, J. Fan, X. Qiang, X. Wang, B. Dou and X. Peng, *Chem. Commun.*, 2012, **48**, 2949; (*b*) Y. Huang, P. Zhang, M. Gao, F. Zeng, A. Qin, S. Wu and B. Z. Tang, *Chem. Commun.*, 2016, **52**, 7288; (*c*) L. Zhi, Z. Wang, J. Liu, W. Liu, H. Zhang, F. Chen and B. Wang, *Nanoscale*, 2015, **7**, 11712; (*d*) J. T. Hou, K. Li, J. Yang, K. K. Yu, Y. X. Liao, Y. Z. Ran, Y. H. Liu, X. D. Zhou and X. Q. Yu, *Chem. Commun.*, 2015, **51**, 6781; (*e*) K. Y. Zhang, J. Zhang, Y. Liu, S. Liu, P. Zhang, Q. Zhao, Y. Tanga and W. Huang, *Chem. Sci.*, 2015, **6**, 301; (*f*)

L. Yuan, W. Lin, Y. Xie, B. Chen and J. Song, *Chem.–Eur. J.*, 2012, **18**, 2700; (*g*) S. Goswami, A. Manna, S. Paul, C. K. Quah and H. K. Fun, *Chem. Commun.*, 2013, **49**, 11656; (*h*) L. Long, D. Zhang, X. Li, J. Zhang, C. Zhang and L. Zhou, *Anal. Chim. Acta*, 2013, **775**, 100; (*i*) L. Wang, L. Long, L. Zhou, Y. Wu, C. Zhang, Z. Han, J. Wang and Z. Da, *RSC Adv.*, 2014, **4**, 59535; (*j*) L. Long, Y. Wu, L. Wang, A. Gong, F. Hu and C. Zhang, *Chem. Commun.*, 2015, **51**, 10435.

10 N. Ponsa, J. Sattabongkot, P. Kittayapong, N. Eikarat and R. E. Coleman, *Am. J. Trop. Med. Hyg.*, 2003, **69**, 542.

11 D. R. Hill, J. K. Baird, M. E. Parise, L. S. Lewis and E. T. Ryan, *Am. J. Trop. Med. Hyg.*, 2006, **75**, 402.

12 *Practical Chemotherapy of Malaria*, World Health Organization Technical Report Series no. 805, World Health Organization, Geneva, 1990, p. 128.

13 *Leishmaniasis Fact sheet No. 375*, World Health Organization, January 2014.

14 (*a*) S. Dröse and U. Brandt, *J. Biol. Chem.*, 2008, **283**, 21649; (*b*) A. Mehta and C. Shaha, *J. Biol. Chem.*, 2004, **279**, 11798.

15 (*a*) M. Shortreed, R. Kopelman, M. Kuhn and B. Hoyland, *Anal. Chem.*, 1996, **68**, 1414; (*b*) N. Sharma, S. I. Reja, V. Bhalla and M. Kumar, *Dalton Trans.*, 2014, **43**, 15929.

16 C. Mancini, A. Kairdolf, M. Smith and S. Nie, *J. Am. Chem. Soc.*, 2008, **130**, 10836.

17 (*a*) E. B. Love and L. Tsai, *Synth. Commun.*, 1992, **22**, 3101; (*b*) X. Liu, A. Zheng, D. Luan, X. Wang, F. Kong, L. Tong, K. Xu and B. Tang, *Anal. Chem.*, 2017, **89**, 1787.

18 M. Whiteman and J. P. E. Spencer, *Biochem. Biophys. Res. Commun.*, 2008, **371**, 50.

19 (*a*) J. Fan, H. Mu, H. Zhu, J. Du, N. Jiang, J. Wang and X. Peng, *Ind. Eng. Chem. Res.*, 2015, **54**, 8842; (*b*) C. Wang, H. Ji, M. Li, L. Cai, Z. Wang, Q. Li and Z. Li, *Faraday Discuss.*, 2017, **196**, 427.

20 K. Setsukinai, Y. Urano, K. Kakinuma, H. J. Majima and T. Nagano, *J. Biol. Chem.*, 2003, **278**, 3170.

21 N. Umezawa, K. Tanaka, Y. Urano, K. Kikuchi, T. Higuchi and T. Nagano, *Angew. Chem., Int. Ed.*, 1999, **38**, 2899.

22 (*a*) Z. Sun, F. Liu, Y. Chen, P. K. H. Tam and D. Yang, *Org. Lett.*, 2008, **10**, 2171; (*b*) Y. Yang, H. J. Cho, J. Lee, I. Shin and J. Tae, *Org. Lett.*, 2009, **11**, 859.

23 Y. Shiraishi, K. Tanaka, E. Shirakawa, Y. Sugano, S. Ichikawa, S. Tanaka and T. Hirai, *Angew. Chem., Int. Ed.*, 2013, **52**, 8304.

24 Y. Shiraishi, M. Nakamura, K. Yamamoto and T. Hirai, *Chem. Commun.*, 2014, **50**, 11583.

25 (*a*) A. Proutiere, E. Megnassan and H. Hucteau, *J. Phys. Chem.*, 1992, **96**, 3485; (*b*) B. Bag and P. K. Bharadwaj, *J. Phys. Chem. B*, 2005, **109**, 4377.

26 R. E. Stratmann, G. E. Scuseria and M. J. Frisch, *J. Chem. Phys.*, 1998, **109**, 8218.

27 M. Cossi, V. Barone, R. Cammi and J. Tomasi, *Chem. Phys. Lett.*, 1996, **255**, 327.